Rapid Communications

Distinct reduction of Knight shift in superconducting state of Sr_2RuO_4 under uniaxial strain

Austin W. Lindquist[1] and Hae-Young Kee[1,2,*]

[1]*Department of Physics and Center for Quantum Materials, University of Toronto, 60 St. George St., Toronto, Ontario, Canada M5S 1A7*

[2]*Canadian Institute for Advanced Research, Toronto, Ontario, Canada M5G 1Z8*

(Received 4 December 2019; revised 11 May 2020; accepted 22 July 2020; published 31 August 2020)

Shortly after the discovery of superconductivity in Sr_2RuO_4, spin-triplet pairing was proposed and further corroborated by a constant Knight shift (K) across the transition temperature (T_c). However, a recent experiment observed a drop in K at T_c which becomes larger under uniaxial strain, ruling out several spin-triplet scenarios. Here we show that even parity interorbital spin-triplet pairing can feature a d vector that rotates when uniaxial strain is applied, leading to a larger drop in the spin polarization perpendicular to the strain direction, distinct from spin-singlet pairing. We propose that anisotropic spin polarization under strain will ultimately differentiate triplet versus singlet pairing.

DOI: 10.1103/PhysRevResearch.2.032055

Introduction. The discovery of superconductivity in Sr_2RuO_4 [1] has had great attention over the past two decades. It has been considered the best solid-state system which exhibits a time-reversal symmetry breaking p-wave spin-triplet pairing analog of the A phase in ^{3}He [2]. The microscopic route to the spin-triplet pairing in ^{3}He is ferromagnetic fluctuations [3]. Since a sister compound, $SrRuO_3$, is a ferromagnetic metal, the $p + ip$ spin triplet pairing proposed by Rice and Sigrist [4] was a promising candidate. Earlier experiments of nuclear magnetic resonance (NMR) and μSR had corroborated this proposal, because no change in the NMR Knight shift [5] and a broken time reversal symmetry signal across T_c in μSR [6] are consistent with the order parameter. However, a scanning magnetic imaging [7] measurement showed a null signal of the associated chiral supercurrent, which does not support the chiral p-wave spin-triplet pairing. Since then, the pairing symmetry of Sr_2RuO_4 has remained a mystery with controversial experimental results [8–11].

Recently, Pustogow *et al.* [12] made an important breakthrough in determining the spin component of the order parameter, as they reported a 20%–50% drop, depending on the field strength, in the spin polarization M_s below T_c in unstrained samples in contrast to the earlier NMR reports [5]. When the sample is strained along the a axis, the spin polarization along the b axis drops almost 75%. This rules out the d vector along the c axis as in the chiral pairing proposal [4]. Since the no-change Knight shift across T_c has been the strong piece of evidence of a spin triplet, this observation may rule out several spin-triplet pairings including the d vector along the c axis, and potentially in the ab plane, depending on the magnitude of the decrease observed, as listed in Ref. [12].

Here we show that orbital-singlet spin-triplet (OSST) pairings [13] exhibit a significant reduction in the spin polarization under strain, and it becomes anisotropic relative to the strain direction. For OSST pairings the d vector is locked in momentum space via spin-orbit coupling (SOC) as shown in Fig. 1. When the uniaxial strain is applied, the strength of the pairing is enhanced due to the van Hove singularity (vHS), which is true for both spin singlet and triplet. However, for an OSST with an in-plane d vector, there is an important additional effect of uniaxial strain. It not only enhances the magnitude of the pairing, but also *rotates* the direction of the d vector as shown in Fig. 1(b), because the strain changes the composition of orbitals which then affects the d vector direction. The d vector rotation creates an anisotropy between spin polarizations parallel versus perpendicular to the strain direction. When the strain is applied along the a axis, the d vector rotates towards the b axis as shown by the red arrows in Fig. 1, leading to a larger drop in the spin-polarization along the b axis than that of the unstrained case, as reported in Ref. [12]. With the same strain condition, the a-axis polarization drop should be smaller. For a singlet, the two spin polarizations are the same. Thus we propose a NMR Knight shift experiment with the reasonably large field (but below the 1.5 T upper critical field) along the a axis under the a-axis strain, to be compared with the b-axis polarization. This will ultimately differentiate spin-triplet versus -singlet pairings.

Below we formulate the proposed idea using a model which consists of a Kanamori interaction and a t_{2g} tight binding model with SOC. While the atomic SOC leading to an s-wave gap is used for clarity, it can be generalized by including momentum dependent SOC terms leading to any even-parity OSST pairing (such as d-wave or g-wave).

Microscopic Hamiltonian. Sr_2RuO_4 is a multiorbital system with non-negligible SOC. The orbital degrees of freedom allow for four distinct pairings which satisfy the antisymmetric fermion wave function requirement, i.e., $\hat{\Delta}(\mathbf{k}) = -\hat{\Delta}^T(-\mathbf{k})$. The four types are: (i) even-parity intraorbital (or interorbital-triplet) spin singlet ($\hat{\phi}_a$ or $\hat{\phi}_v$), (ii) odd-parity

*hykee@physics.utoronto.ca

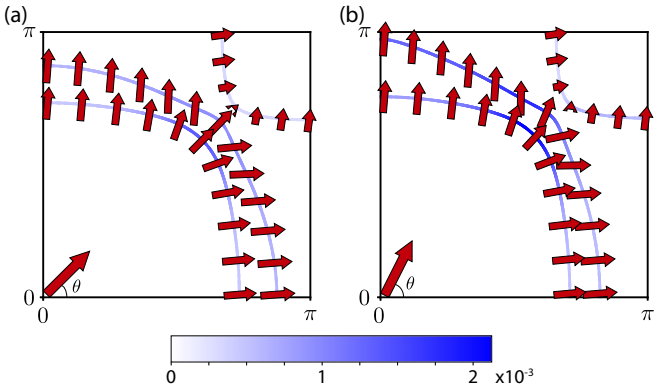

FIG. 1. The red arrows at representative momenta show the d vector of inter-orbital spin triplet pairing for (a) unstrained and (b) uniaxial-strain along a axis. This transforms to intraband pseudospin-singlet pairing on the FS and inter-band pairings (see the main text for details). The d vector rotation occurs the most in the diagonal direction of the Brillouin zone. The length of each arrow represents the in-plane component; the shorter the arrow, the bigger the c-axis component. Note that the arrows with an inverted tail correspond to a vector primarily along the c axis. The blue color on the FS denotes the size of gap. The red arrow at the bottom corner of each panel represents the averaged d vector direction projected onto the ab-plane denoted by θ; $\theta = 45^\circ$ and 63° in (a) and (b), respectively.

interorbital-singlet spin singlet, (iii) odd-parity intraorbital (or interorbital-triplet) spin triplet ($\hat{\mathbf{d}}_a$), and (iv) even-parity OSST ($\hat{\mathbf{D}}_\nu$), where ν represents interorbital, and a, intraorbital pairings among t_{2g} [13].

A generic Hamiltonian $H = H_{\rm kin} + H_{\rm SOC} + H_{\rm int}$ consisting of a tight binding model, SOC, and Kanamori interaction is considered. The tight binding and SOC terms are used to reproduce the Fermi surface (FS) reported in Ref. [14], and are listed in Ref. [15]. The underlying FS of three bands, α, β, and γ is reported earlier [16–18], and was further refined in Ref. [14] shown as the solid lines in Fig. 1. The interaction term is given by

$$H_{\rm int} = \frac{U}{2}\sum_{i,a} c^{a\dagger}_{i\sigma} c^{a\dagger}_{i\sigma'} c^{a}_{i\sigma'} c^{a}_{i\sigma} + \frac{V}{2}\sum_{i,a\neq b} c^{a\dagger}_{i\sigma} c^{b\dagger}_{i\sigma'} c^{b}_{i\sigma'} c^{a}_{i\sigma} + \frac{J_H}{2}\sum_{i,a\neq b} c^{a\dagger}_{i\sigma} c^{b\dagger}_{i\sigma'} c^{a}_{i\sigma'} c^{b}_{i\sigma} + \frac{J_H}{2}\sum_{i,a\neq b} c^{a\dagger}_{i\sigma} c^{a\dagger}_{i\sigma'} c^{b}_{i\sigma'} c^{b}_{i\sigma}, \quad (1)$$

with Hubbard interaction, U, and Hund's coupling, J_H, where $V = U - 2J_H$, and where a and b represent the t_{2g} orbitals (yz, xz, xy). This can be expressed in terms of pairing order parameters, including the OSST parameters, which appear as

$$\frac{H_{\rm eff}}{2N} = (V - J_H)\sum_{\nu} \hat{\mathbf{D}}^\dagger_\nu(\mathbf{q}) \cdot \hat{\mathbf{D}}_\nu(\mathbf{q}), \quad (2)$$

where $\hat{D}^{l\dagger}_\nu$ is given by

$$\hat{D}^{l\dagger}_\nu(\mathbf{q}) = \frac{1}{4N}\sum_{\mathbf{k}} c^{a\dagger}_{\mathbf{k}\sigma}[i\hat{\sigma}^y\hat{\sigma}^l]_{\sigma\sigma'}[\hat{\lambda}_\nu]_{ab} c^{b\dagger}_{-\mathbf{k}+\mathbf{q}\sigma'}, \quad (3)$$

with $l = x, y, z$. $\hat{\lambda}_\nu$ are 3×3 antisymmetric matrices in the orbital basis under the exchange of the t_{2g} orbitals for three

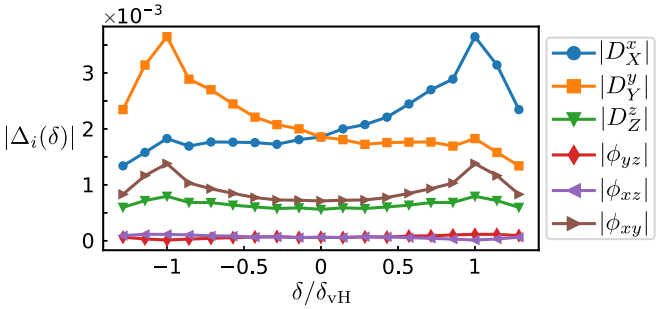

FIG. 2. Magnitude of the finite components of $\mathbf{D}_\nu$ and ϕ_a as a function of strain δ showing roughly quadratic behavior of the gap size in δ with a maximum at the vHS as expected. Note that D^x_X/D^y_Y and ϕ_{xz}/ϕ_{yz} show the expected asymmetry with respect to $\pm\delta$.

different interorbital matrices denoted with $\nu = X$ (between xz and xy orbitals), Y (yz and xy), and Z (xz and yz). Their expressions are given in Ref. [15]. The full form of the interaction written in terms of pairing order parameters, including induced intra orbital spin singlets ϕ_a, and interorbital-triplet spin singlets, both of which appear with repulsive interactions, are also given in Ref. [15]. The OSST channel has an attractive interaction for $3J_H > U$, and while this is larger than most values of Hund's coupling in $4d$ transition metals, where J_H is about 20%–30% of U [19], recent studies going beyond mean-field theory support OSST pairing originating from Hund's coupling without the strict condition of $3J_H > U$ [20–23]. The direction of the d vector is determined by the SOC [13,24], with order parameters belonging to the A_{1g} representation for atomic SOC [25–27]. The importance of the SOC in Sr_2RuO_4 was addressed earlier [13,28–31], and recently re-emphasized [14].

Pairing gap under strain. Since the OSST pairing corresponds to pairing between orbitals with different energies at $\mathbf{k}$ and $-\mathbf{k}$, we consider the possibility of finite momentum pairing, i.e., FFLO state. Using a self-consistent mean-field theory, we find the zero-momentum $\mathbf{q} = 0$ state is always the lowest state despite the pairing between different orbitals. However, the pairing amplitude appears to be extremely small as shown in Fig. 2 with the magnitudes of the $\mathbf{D}_\nu$ and induced intraband spin singlets, ϕ_a. They are thousands of times smaller than the t_{2g} bandwidth, even though the attractive interaction is reasonably large. We set $3J_H - U = 0.5$ for the current results, and the mean-field theory in general overestimates the gap size. The interorbital pairing would appear to require a finite q value to produce a gap on the FS without orbital hybridization or SOC. However, when the atomic SOC is finite the OSST pairing projected onto the band basis transforms into *intraband* pseudospin-singlet pairing on the FS, denoted by $\tilde{D}_i$ where $i = \alpha$, β, and γ in the quasiparticle dispersion shown in Fig. S1. The quasiparticle dispersion represents strongly anisotropic gaps, which are very small in size, both at and below the FS. This suggests that when the bandwidth is renormalized by electronic correlations, and becomes narrower, the OSST is further favoured. A recent dynamical mean-field theory reported a strong mass renormalization of the bands [32], which would also enhance the OSST pairing.

To study the uniaxial strain effects, we change the ratio of the hopping integrals along the a and b axes such that

$t_{jx} = (1-\delta)t_j$ and $t_{jy} = (1+\delta)t_j$ for $j = 1, 2, 3$. Uniaxial strain along the a axis corresponds to $\delta < 0$. The change of different order parameters as a function of δ is shown in Fig. 2. The pairing gap is roughly quadratic in δ as expected from the even parity pairing. While D_X^x and D_Y^y exhibit opposite behavior under strain, these A_{1g} solutions do not exhibit a split transition under strain [25]. When the γ band touches the vHS around $\delta = \pm 0.07$, the pairing amplitude is peaked. Since mean-field theory causes the gap to be proportional to the transition temperature, T_c is also peaked as reported in Refs. [33,34]. The overall gap size is minuscule in comparison to the energy scale of the kinetic and potential terms as discussed above.

Rotation of the d vector under uniaxial strain. For spin-triplet pairing, the d vector represents the direction along which the spin projection of the condensed pair has eigenvalue zero [3]. When SOC is finite, the mean-field solutions find the pinning of the d vector depending on the interorbital composition via SOC. For the pairing between xz and xy orbitals, the d vector points along the x direction (represented by D_X^x), yz and xy along the y direction (D_Y^y), and xz and yz along the z axis (D_Z^z). The x, y, and z axes are the same as the crystallographic axes of a, b, and c, as Sr_2RuO_4 is a tetragonal lattice. The d vector changes in momentum space as shown in Fig. 1(a), as the orbital composition changes along the FS. The red arrows represent the d vector directions. The shorter the length of arrow, the bigger the c-axis component of the d vector. There is a finite d vector at every momentum point, and on average it is finite in all directions leading to a reduction of the spin polarization in all directions.

In the absence of strain, due to the tetragonal symmetry, there is a $\frac{\pi}{2}$ rotational symmetry between $\hat{D}^x$ and $\hat{D}^y$. This leads to the same reduction of the spin polarization along the a and b axes (and any other directions related to the symmetry of the tetragonal lattice). However, when the uniaxial strain is applied, the orbital composition changes mainly around X and Y regions of the Brillouin Zone (BZ) as shown by the underlying FS in Fig. 1(b). Most importantly, the yz orbital contribution to all bands increases, causing the d vector at every momentum to rotate towards the b-axis, with the most change occurring around the diagonal direction of the BZ. This will then affect the magnitude of the spin polarization in the superconducting state, and generates a directional dependence, which we show below.

Spin polarization under strain. The magnetic susceptibility χ_{jj} measured by the NMR Knight shift is given by $\partial M_j/\partial B_j$ where $\mathbf{M}$ is the magnetization, $\mathbf{B}$ is an external magnetic field, and $j = x, y, z$. Using a Zeeman coupling $H_{\text{Zeeman}} = \sum_i (\mathbf{L}_i + g\mathbf{S}_i)\cdot\mathbf{B}$, we compute the contribution from the spin polarization at a site i, in the j direction, $\langle S_i\rangle_j$, assuming the orbital contribution, which has been suggested to be small [35], can be separated. We also compute the contribution from the orbital magnetization $\langle L_i\rangle$, and there is a slight drop in the superconducting state as shown in Fig. S2 in Ref. [15]. The results are shown in Fig. 3, which shows the spin magnetization along the x and y directions as the strain changes. Here we plot the ratio between the strained values, and the normal state unstrained cases.

A conventional spin triplet will feature a Knight shift which appears the same as a singlet for the field parallel to the d vector and shows no change from the normal state for the field perpendicular to the d vector. On the other hand, OSST pairing leads to intraband pseudospin-singlet pairing occuring near the FS, and interband spin triplet away from the FS. Thus, the low field response behavior is due primarily to the intraband pairing [36], which causes a large drop in the approximately isotropic Knight shift as shown in Fig. 3(a). However, by increasing the field such that it is a significant fraction of the gap size ($\mathbf{B} \sim 0.2|\mathbf{D}_0|$), the interband pairing with d vector rotation is observable, and such rotation results in an anisotropic Knight shift under strain as shown in Fig. 3(b). Thus, for OSST, the Knight shift is more affected by intraband pseudospin-singlet pairing at low fields, and interband pairing at higher fields. As expected from the d vector rotation under the a-axis strain, we find a greater drop in the magnetization from the normal to superconducting state in the y direction compared with the x direction, with a difference of about 20% for the larger field value. The magnetization in the x direction also drops under strain due to the strain bringing the sample deeper into the superconducting state. The value of the drop from the normal to superconducting state depends on the value of the SOC, and by decreasing the SOC, the Knight shift drop and the anisotropy under strain enhance further.

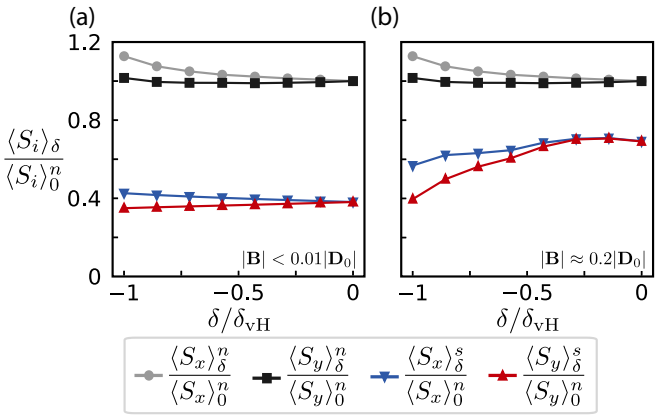

FIG. 3. The spin magnetization $\mathbf{S}$ in the normal (n) and superconducting (s) states, normalized to the zero-strain normal state value, for (a) a small field where $\mathbf{S}$ is linear in B with $B < 1\%$ of $|\mathbf{D}_0|$ where $|\mathbf{D}_0|$ is $|\mathbf{D}|$ at $\delta = 0$, and (b) a field comparable to the gap minimum, where $\mathbf{S}$ is no longer linear, $B \approx 0.2 \times |\mathbf{D}_0|$.

Extending to three-dimensional bands. Sr_2RuO_4 has a layered structure, and one expects to see more k_z dispersion of the bands originating from xz and yz orbitals due to their shape, and less dispersion from the xy orbital. The momentum dependent t_{2g}-orbital projection of the wave function for the α, β and γ bands on the three-dimensional FS was reported [31], which is consistent with the three dimensional (3D) tight binding model constructed in Ref. [37]. The β and γ bands still have significant overlap of xy and one dimensional (1D) orbitals, even though detailed composition depends on k_z as shown in Ref. [31], while the α band is mainly made of 1D orbitals. Thus the above analysis done in the two-dimensional (2D) system can be generalized to a layered three-dimensional system. The qualitative uniaxial strain effect, i.e., the relative directional dependence of the spin polarization under a uniaxial strain, is independent of the details of c-axis hopping

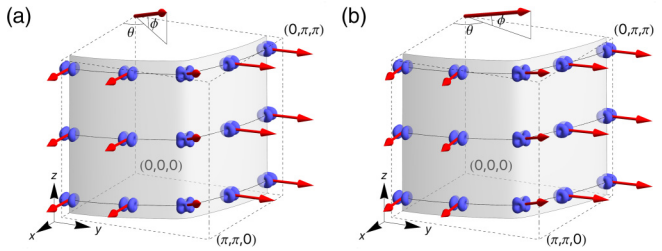

FIG. 4. The d vectors on the 3D γ-band FS are shown at various momentum points for (a) no strain and (b) strain along the a axis. The average d vector indicated by the red arrow at the top corner shows the rotation of the d vector denoted by (θ, ϕ) towards b axis and slightly c axis under the a-axis uniaxial strain. Similar to the 2D case, most of the rotation of d-vector occurs near the diagonal direction of the BZ.

parameters, even though the quantitative drop may depend on the strength of the hopping parameters. Using the tight binding parameters in Ref. [37], we found the d vector directions are similar to the 2D case. The angle ϕ represents the tilting from the ab plane, which is about $17 - 19^\circ$ depending on k_z. A clear rotation of the averaged d vector is shown as a red arrow in a top corner in Fig. 4, and the main conclusion of the d vector rotation can be generalized to the 3D model including the layer coupling.

Discussion and summary. In multiorbital systems, orbital degrees of freedom extend the types of superconducting pairings. Even-parity spin-triplet pairings are allowed when the pairing occurs between different orbitals with the antisymmetric fermionic wavefunction condition, i.e., orbital singlets. In the band basis, this maps to interband, and intraband pairings when SOC is finite [13]. SOC in the OSST pairing determines the intraband gap on the FS. The idea of OSST pairing is not limited to the atomic (s-wave) SOC leading to an s-wave gap with the A_{1g} representation. It can be generalized to the momentum dependent SOC terms resulting in higher order OSST terms such as d- and g-wave, which can explain the nodal structure of the gap, as well as recent experiments suggesting a multicomponent order parameter based on the elastic moduli [38,39]. These experiments have contributed to a recent proposal of a combined d- and g-wave gap [40]. Within the OSST pairing scenario, the multicomponent order parameter can be found using the momentum dependent SOC including d- and g-wave SOC terms. We find a finite d- and g-wave gap structure with the d- and g-wave SOC terms as expected. However, a self-consistent solution to determine the energetics of all possible pairings is the subject of future work.

Odd-parity, intraorbital (and interorbital triplet) spin-triplet pairing is also possible when the ferromagnetic interaction is extended to further neigbour site [25], even though the impact of the increased density of states via the vHS is drastically reduced due to the $\sin(nk_{x/y})$ form factor, where n is an integer representing the nearest and further nearest neighbor distance. An interaction of this form has been shown to give a helical order parameter [2,4,41]. We consider this possibility and show that there is still potentially an asymmetry of the in-plane magnetic response for an in-plane d vector in Ref. [15]. While recent neutron scattering experiments and DMFT calculations do not support ferromagnetic spin fluctuations giving rise to spin-triplet pairing [42,43], this triplet leads to an anisotropy, but cannot reproduce the $>50\%$ drop in the NMR response, with an $\sim 40\%$ or smaller drop in the NMR response for all field strengths, unlike the OSST pairing. For this odd-parity pairing, the drop in the Knight shift with no SOC is 50%, and the inclusion of SOC decreases the magnitude of the drop. Therefore, if an anisotropy in the Knight shift is observed, the odd-parity spin-triplet solutions must also be considered as possible explanations, however, the exact value of the drop in the Knight shift will provide important evidence for identifying the pairing states. For unstrained samples, the impact of pulse energy is stronger than in the case of strained samples as stated in Ref. [12], and further experimental analysis is required to determine if the reduction is more than 50% in the unstrained case.

Another consequence of SOC is a complex order parameter. Generally, the order parameter with the SOC induced spin-singlet components can be written with a phase factor, $\hat{\mathbf{D}} + e^{i\theta}\hat{\phi}$ (where $\hat{\mathbf{D}}$ is defined to be imaginary such that it is even under TR), where the relative phase between the two is determined by the atomic SOC [13], and $\theta = 0$ for uniform SOC. Despite not breaking time-reversal symmetry, as the time-reversal operator maps the order parameter to itself, the order parameter near impurities may change its relative phase from $\theta = 0$ leading to nontrivial effects. Thus, the multicomponent order parameter may be important to understand the μSR [6] and Josephson junction [44] results. This is an open topic for future study.

In summary, we showed OSST pairing with SOC leads to a significant reduction of the Knight shift and an anisotropic Knight shift response under uniaxial strain, which can ultimately be used to differentiate spin-triplet from spin-singlet pairing in Sr_2RuO_4. When the strain is applied along the a axis, interorbital pairing involving d_{yz} and d_{xy} is further enhanced leading to a rotation of the d vector towards the b axis. As a consequence of the d vector rotation, the Knight shift becomes anisotropic relative to the strain axis. It has more drop in the magnetization when the magnetic field is perpendicular to the strain and less when the field is parallel to the strain. Such anisotropy is not expected in the spin singlet, thus we propose the Knight shift measurement with the field along the a axis, which can be compared with the data presented in Ref. [12]. This will ultimately determine a long-standing debate of a possible spin-triplet pairing in Sr_2RuO_4. This idea can also be extended to other multiorbital systems with significant Hund's coupling and SOC.

Acknowledgments. This work was supported by the Natural Sciences and Engineering Research Council of Canada Discovery Grant 2016-06089, and the Center for Quantum Materials at the University of Toronto.

[1] Y. Maeno, H. Hashimoto, K. Yoshida, S. Nishizaki, T. Fujita, J. G. Bednorz, and F. Lichtenberg, Nature (London) **372**, 532 (1994).

[2] A. P. Mackenzie and Y. Maeno, Rev. Mod. Phys. **75**, 657 (2003).

[3] A. J. Leggett, Rev. Mod. Phys. **47**, 331 (1975).

[4] T. M. Rice and M. Sigrist, J. Phys.: Condens. Matter **7**, L643 (1995).

[5] K. Ishida, H. Mukuda, Y. Kitaoka, K. Asayama, Z. Q. Mao, Y. Mori, and Y. Maeno, Nature (London) **396**, 658 (1998).

[6] G. M. Luke, Y. Fudamoto, K. M. Kojima, M. I. Larkin, J. Merrin, B. Nachumi, Y. J. Uemura, Y. Maeno, Z. Q. Mao, Y. Mori, H. Nakamura, and M. Sigrist, Nature (London) **394**, 558 (1998).

[7] P. G. Björnsson, Y. Maeno, M. E. Huber, and K. A. Moler, Phys. Rev. B **72**, 012504 (2005).

[8] K. D. Nelson, Z. Mao, Y. Maeno, and Y. Liu, Science **306**, 1151 (2004).

[9] J. Jang, D. G. Ferguson, V. Vakaryuk, R. Budakian, S. B. Chung, P. M. Goldbart, and Y. Maeno, Science **331**, 186 (2011).

[10] C. Kallin, Rep. Prog. Phys. **75**, 042501 (2012).

[11] A. P. Mackenzie, T. Scaffidi, C. W. Hicks, and Y. Maeno, npj Quantum Mater. **2**, 40 (2017).

[12] A. Pustogow, Y. Luo, A. Chronister, Y.-S. Su, D. A. Sokolov, F. Jerzembeck, A. P. Mackenzie, C. W. Hicks, N. Kikugawa, S. Raghu *et al.*, Nature (London) **574**, 72 (2019).

[13] C. M. Puetter and H.-Y. Kee, Europhys. Lett. **98**, 27010 (2012).

[14] A. Tamai, M. Zingl, E. Rozbicki, E. Cappelli, S. Riccò, A. de la Torre, S. McKeown Walker, F. Y. Bruno, P. D. C. King, W. Meevasana, M. Shi, M. Radović, N. C. Plumb, A. S. Gibbs, A. P. Mackenzie, C. Berthod, H. U. R. Strand, M. Kim, A. Georges, and F. Baumberger, Phys. Rev. X **9**, 021048 (2019).

[15] See Supplemental Material at http://link.aps.org/supplemental/10.1103/PhysRevResearch.2.032055 for details of the full Hamiltonian, the quasiparticle dispersion, and the magnetization calculations, as well as additional calculations for the orbital magnetization and odd-parity pairing.

[16] A. P. Mackenzie, S. R. Julian, A. J. Diver, G. J. McMullan, M. P. Ray, G. G. Lonzarich, Y. Maeno, S. Nishizaki, and T. Fujita, Phys. Rev. Lett. **76**, 3786 (1996).

[17] C. Bergemann, S. R. Julian, A. P. Mackenzie, S. NishiZaki, and Y. Maeno, Phys. Rev. Lett. **84**, 2662 (2000).

[18] A. Damascelli, D. H. Lu, K. M. Shen, N. P. Armitage, F. Ronning, D. L. Feng, C. Kim, Z.-X. Shen, T. Kimura, Y. Tokura, Z. Q. Mao, and Y. Maeno, Phys. Rev. Lett. **85**, 5194 (2000).

[19] A. Georges, L. d. Medici, and J. Mravlje, Ann. Rev. Condens. Matter Phys. **4**, 137 (2013).

[20] S. Hoshino and P. Werner, Phys. Rev. Lett. **115**, 247001 (2015).

[21] S. Hoshino and P. Werner, Phys. Rev. B **93**, 155161 (2016).

[22] O. Gingras, R. Nourafkan, A.-M. S. Tremblay, and M. Côté, Phys. Rev. Lett. **123**, 217005 (2019).

[23] F. B. Kugler, M. Zingl, H. U. R. Strand, S.-S. B. Lee, J. von Delft, and A. Georges, Phys. Rev. Lett. **124**, 016401 (2020).

[24] H. G. Suh, H. Menke, P. M. R. Brydon, C. Timm, A. Ramires, and D. F. Agterberg, Phys. Rev. Research **2**, 032023 (2020).

[25] A. Ramires and M. Sigrist, Phys. Rev. B **100**, 104501 (2019).

[26] W. Huang, Y. Zhou, and H. Yao, Phys. Rev. B **100**, 134506 (2019).

[27] A. K. C. Cheung and D. F. Agterberg, Phys. Rev. B **99**, 024516 (2019).

[28] E. Pavarini and I. I. Mazin, Phys. Rev. B **74**, 035115 (2006).

[29] M. W. Haverkort, I. S. Elfimov, L. H. Tjeng, G. A. Sawatzky, and A. Damascelli, Phys. Rev. Lett. **101**, 026406 (2008).

[30] E. J. Rozbicki, J. F. Annett, J.-R. Souquet, and A. P. Mackenzie, J. Phys.: Condens. Matter **23**, 094201 (2011).

[31] C. N. Veenstra, Z.-H. Zhu, M. Raichle, B. M. Ludbrook, A. Nicolaou, B. Slomski, G. Landolt, S. Kittaka, Y. Maeno, J. H. Dil, I. S. Elfimov, M. W. Haverkort, and A. Damascelli, Phys. Rev. Lett. **112**, 127002 (2014).

[32] M. Kim, J. Mravlje, M. Ferrero, O. Parcollet, and A. Georges, Phys. Rev. Lett. **120**, 126401 (2018).

[33] C. W. Hicks, D. O. Brodsky, E. A. Yelland, A. S. Gibbs, J. a. N. Bruin, M. E. Barber, S. D. Edkins, K. Nishimura, S. Yonezawa, Y. Maeno, and A. P. Mackenzie, Science **344**, 283 (2014).

[34] A. Steppke, L. Zhao, M. E. Barber, T. Scaffidi, F. Jerzembeck, H. Rosner, A. S. Gibbs, Y. Maeno, S. H. Simon, A. P. Mackenzie, and C. W. Hicks, Science **355**, eaaf9398 (2017).

[35] K. Ishida, M. Manago, K. Kinjo, and Y. Maeno, J. Phys. Soc. Jpn. **89**, 034712 (2020).

[36] Y. Yu, A. K. C. Cheung, S. Raghu, and D. F. Agterberg, Phys. Rev. B **98**, 184507 (2018).

[37] H. S. Røising, T. Scaffidi, F. Flicker, G. F. Lange, and S. H. Simon, Phys. Rev. Research **1**, 033108 (2019).

[38] S. Benhabib, C. Lupien, I. Paul, L. Berges, M. Dion, M. Nardone, A. Zitouni, Z. Q. Mao, Y. Maeno, A. Georges, L. Taillefer, and C. Proust, arXiv:2002.05916.

[39] S. Ghosh, A. Shekhter, F. Jerzembeck, N. Kikugawa, D. A. Sokolov, M. Brando, A. P. Mackenzie, C. W. Hicks, and B. J. Ramshaw, arXiv:2002.06130.

[40] S. A. Kivelson, A. C. Yuan, B. Ramshaw, and R. Thomale, npj Quantum Mater. **5**, 43 (2020).

[41] K. K. Ng and M. Sigrist, Europhys. Lett. **49**, 473 (2000).

[42] P. Steffens, Y. Sidis, J. Kulda, Z. Q. Mao, Y. Maeno, I. I. Mazin, and M. Braden, Phys. Rev. Lett. **122**, 047004 (2019).

[43] H. U. R. Strand, M. Zingl, N. Wentzell, O. Parcollet, and A. Georges, Phys. Rev. B **100**, 125120 (2019).

[44] S. Kashiwaya, K. Saitoh, H. Kashiwaya, M. Koyanagi, M. Sato, K. Yada, Y. Tanaka, and Y. Maeno, Phys. Rev. B **100**, 094530 (2019).